Focus grid generation by in-line holography

Jigang Wu,[1,*] Lap Man Lee,[2] and Changhuei Yang[1,2]

[1]*Department of Electrical Engineering, California Institute of Technology, 1200 E California Blvd., Pasadena, CA 91125, USA*

[2]*Department of Bioengineering, California Institute of Technology, 1200 E California Blvd., Pasadena, CA 91125, USA*

**jigang@caltech.edu*

Abstract: We describe a simple way to generate a wide-area high-resolution focus grid by in-line holography and study the factors that impacts its quality. In our holographic recording setup, the reference beam was the direct transmission of the incoming collimated laser beam through a mask coating with thin metal film, and the sample beam was the transmission of the laser through small apertures fabricated on the mask. The interference of the two beams was then recorded by a holographic plate positioned behind the mask. Compared with other recording schemes, the in-line holography scheme has many distinct advantages and is more suitable for generating a wide-area focus grid. We explored the dependence of diffraction quality, including reconstructed focus spot intensity and spot size, on different parameters for recording, such as optical density of the metal film, size of the apertures, and focal lengths. A wide-area focus grid (170 x 138 spots with area 5.1 mm x 4.1 mm) was recorded using the in-line holography scheme for a demonstration.

OCIS codes: (090.0900) Holography; (090.2890) Holographic optical element.

References and links

1. R. Gräf, J. Rietdorf, and T. Zimmermann, "Live cell spinning disk microscopy," Adv. Biochem. Eng. Biotechnol. **95**, 57–75 (2005).
2. J. Bewersdorf, R. Pick, and S. W. Hell, "Multifocal multiphoton microscopy," Opt. Lett. **23**(9), 655–657 (1998).
3. P. M. Lundquist, C. F. Zhong, P. Zhao, A. B. Tomaney, P. S. Peluso, J. Dixon, B. Bettman, Y. Lacroix, D. P. Kwo, E. McCullough, M. Maxham, K. Hester, P. McNitt, D. M. Grey, C. Henriquez, M. Foquet, S. W. Turner, and D. Zaccarin, "Parallel confocal detection of single molecules in real time," Opt. Lett. **33**(9), 1026–1028 (2008).
4. J. Ho, A. V. Parwani, D. M. Jukic, Y. Yagi, L. Anthony, and J. R. Gilbertson, "Use of whole slide imaging in surgical pathology quality assurance: design and pilot validation studies," Hum. Pathol. **37**(3), 322–331 (2006).
5. M. Oheim, "High-throughput microscopy must re-invent the microscope rather than speed up its functions," Br. J. Pharmacol. **152**(1), 1–4 (2007).
6. J. Wu, X. Cui, G. Zheng, Y. M. Yang, L. M. Lee, and C. Yang, "A wide field-of-view microscope based on holographic focus grid illumination," (accepted by Opt. Lett.).
7. F. Kalkum, S. Broch, T. Brands, and K. Buse, "Holographic phase conjugation through a sub-wavelength hole," Appl. Phys. B **95**(3), 637–645 (2009).
8. W. Liu, and D. Psaltis, "Pixel size limit in holographic memories," Opt. Lett. **24**(19), 1340–1342 (1999).
9. D. Gabor, "A new microscopic principle," Nature **161**(4098), 777–778 (1948).
10. J. J. Barton, "Removing multiple scattering and twin images from holographic images," Phys. Rev. Lett. **67**(22), 3106–3109 (1991).
11. W. Xu, M. H. Jericho, I. A. Meinertzhagen, and H. J. Kreuzer, "Digital in-line holography for biological applications," Proc. Natl. Acad. Sci. U.S.A. **98**(20), 11301–11305 (2001).
12. V. Moreno, J. F. Roman, and J. R. Salgueiro, "High efficiency diffractive lenses: deduction of kinoform profile," Am. J. Phys. **65**(6), 556–562 (1997).
13. M. H. Horman, and H. H. M. Chau, "Zone plate theory based on holography," Appl. Opt. **6**(2), 317–322 (1967).
14. J. W. Goodman, *Introduction to Fourier Optics* (Roberts & Company Publishers, 3rd edition, 2004), Chap. 9.
15. C. Genet, and T. W. Ebbesen, "Light in tiny holes," Nature **445**(7123), 39–46 (2007).
16. A. K. Richter, and F. P. Carlson, "Holographically generated lens," Appl. Opt. **13**(12), 2924–2930 (1974).
17. H. I. Bjelkhagen, *Silver-halide recording materials for holography and their processing* (Springer, 2nd edition, 1995), Chap. 5.

#128026 - $15.00 USD Received 5 May 2010; revised 27 May 2010; accepted 10 Jun 2010; published 21 Jun 2010

1. Introduction

Focus grid illuminations has been used for multi-beam confocal microscopy [1], multifocal microscopy [2], and single molecule detection [3], etc. In such applications, it is important to generate a tight focus spot for high-resolution imaging, and a small spacing between the focus spots for fast image acquisition speed. Previously, the focus grid is usually generated by using microlens array, diffractive optical elements, or holographic optical elements, along with a microscope objective to achieve the abovementioned characteristics. One disadvantage of these methods is that the area of the focus grid illumination will be limited by the field-of-view of microscope objective, and is thus unsuitable for applications that require wide field-of-view imaging, e.g., whole-slide imaging [4] or high-throughput imaging and sensing [5]. Obviously, to achieve a wider field-of-view, the microscope objective has to be eliminated when generating the focus grid illumination.

An appropriately designed microlens array provides a good alternate solution. The number of elements in such an array can be scaled up arbitrarily. However, there is a significant downside to such a solution – the grid density is typically low. This is because the required numerical apertures for high resolution spots (< 1 μm) necessarily require the focus spot separation and the focal length to be high. For example, to accomplish a focused spot size of 1 μm at a focal distance of 10 mm, each microlens in the array would have to be at least 5 mm in diameter (assuming wavelength of 500 nm). Since the pitch of the focus grid is equal to microlens' diameter, this implies that such an array would have a pitch of 5 mm. This sparse grid density is a significant impediment for most applications. The grid density can potentially be increased by using smaller lenses with shorter focal lengths. However, the required optical surfaces would be more difficult to fabricate and the shorter focal lengths may be restrictive for certain applications.

Interestingly, it is worth noting that the physical lenses are not the only means by which we can focus light. It is also possible to implement a virtual microlens array via holographic recording. An appropriately patterned piece of holographic plate should be able to transform a uniform input coherent light field into a grid of tightly focused light spots. The holographic projection-base approach has two advantages. First, implementation would be simpler and cheaper, as long as we can write the appropriate pattern into the holographic plate. Second, the effective holographic lenses can 'overlap' to a great extent, and, as such, we would be able to achieve a higher focus grid density. Recently, we showed that an appropriately patterned holographic plate can generate light spots of diameter 0.74 μm at a focal distance of 6 mm with a pitch of 30 μm [6]. The corresponding holographic lens diameter is 4.3 mm. This implies that the lens overlap ratio (lens diameter divided by pitch) is 140 (for conventional lenslet array, this ratio is at most 1).

The use of holography to generate a high-resolution focus spot has been demonstrated by several groups via well-designed schemes [7, 8]. In their schemes, the transmission of a tiny aperture was interfered with a reference beam and recorded by holographic materials. This approach can provide high-quality and well-controlled recording.

In-line holography was originally proposed by Gabor more than half a century ago [9] and has been studies extensively since then [10, 11]. In this paper, we show that an in-line holography scheme can be used for generating a wide-area focus grid. In our scheme, as shown in Fig. 1(a), the direct transmission of a collimated laser beam through a semi-transparent mask interferes with the transmission of the laser through an aperture grid fabricated on the semi-transparent mask, and the interference pattern is recorded by a holographic plate. The advantages of our scheme can be summarized as follows: (1) The in-line scheme make the setup insensitive to vibrations and perturbations in the system; (2) The focal length of the focus grid can be adjusted easily and can be short with relative ease; (3) The scheme is suitable for recording large-area aperture grid and thus suitable for achieving large-area focus grid. This paper reports our experimental findings regarding the impact of various implementation parameters on the quality of the recording.

#128026 - $15.00 USD Received 5 May 2010; revised 27 May 2010; accepted 10 Jun 2010; published 21 Jun 2010

The quality of the holographic recording depends on the aperture size, the opacity of the mask and the focal length. The parameter choices for creating an optimal recording are not apparent by simply dissecting the problem analytically. Here, we experimentally show the impact of each major design choice on the recording's properties. This paper will hopefully serves as a guide for researchers looking to create such holographic grids for their respective experiments.

In section 2, we will describe the in-line holography setup for recording the hologram for generating a focus grid and present a theory for calculating the reconstructed focus spot intensity. In section 3, we show a series of experiment that studies the dependence of hologram quality, including reconstructed spot size and diffraction efficiency, on experiment parameters, such as optical density (OD) of the mask, the aperture size, and the focal length. Finally, we summarize our work in section 4.

2. In-line holography setup

The in-line holography setup for recording a hologram that can generate a focus spot (a holographic lens) is shown in Fig. 1(a). The holographic lens is also called a sinusoidal zone plate [12] or a Garbor zone plate [13]. The mask in the setup consists of an aperture patterned on a layer of metal film. When a collimated laser beam shines on the mask, the transmission through the aperture serves as sample wave. The metal film is deliberately made to be thin so that the collimated laser beam can directly transmit through it and be attenuated. The direct transmission of the beam through the metal film then serves as reference wave and interferes with the sample beam and the interference is recorded by a holographic plate positioned at a certain distance behind the mask. In the experiment, we used a silver halide holographic plate.

After exposure, the holographic plate was developed and bleached to produce a phase hologram. A focus spot can then be generated by the holographic reconstruction process, as shown in Fig. 1(b), where a conjugated collimated beam is transformed into a focus spot by the hologram. The focal length of the holographic lens is the same as the distance between the mask and the holographic plate during the recording process.

By replacing the mask with one that is patterned with a grid of apertures, the same process will yield a phase hologram that can render a grid of focus spots.

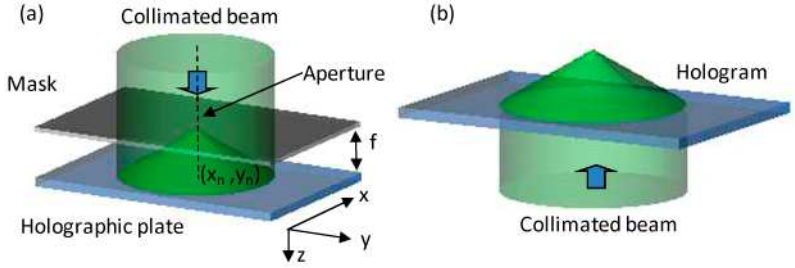

Fig. 1. In-line holography scheme for fabricating a holography lens. (a) Recording of the hologram; (b) Reconstruction of the focus spot.

Considering the sensitivity dynamic range of holographic materials, it is preferable to make the intensity of reference beam comparable to that of the sample beam. This is true if we have only one aperture on the mask. However, for aperture grid on the mask, the interference between the transmissions of different apertures will contribute to the hologram pattern and affect diffraction if the transmissions are comparable to the reference beam transmission. Thus in the recording scheme, it is important to make the intensity of the reference beam much stronger than that of the sample beam so that a reasonable reconstruction can be achieved [14].

The transmission through tiny apertures is generally a complicated problem and defies simple solution without some approximations [15]. An approximate theory for calculating holographically generated lens can be found in Ref [16], where the Fraunhoffer diffraction was used to approximate the transmission through the aperture. Similar to Ref [13], our

#128026 - $15.00 USD Received 5 May 2010; revised 27 May 2010; accepted 10 Jun 2010; published 21 Jun 2010

calculation below is based on the simpler assumption that the sample beam is a combination of spherical waves and the reference beam is a plane wave, since the apertures in our experiment is comparable to the wavelength and much smaller than the focal length. Using paraxial approximation, the sample wave, i.e., the transmission through the aperture grid, can be written as

$$\frac{A_1}{f}\sum_n \exp\left(i\frac{\pi}{f\lambda}[(x-x_n)^2+(y-y_n)^2]\right) \tag{1}$$

where f is the focal length, A_1/f is the amplitude of one hole, (x_n,y_n) is the coordinate of the center of the aperture n, and λ is the laser wavelength. Here we neglect the constant phase shift from propagation along z-direction. Figure 1(a) shows the scheme with aperture n. Thus the interferogram intensity on the holographic plate can be written as:

$$\begin{aligned} I(x) &\approx \left|A_0+\frac{A_1}{f}\sum_n \exp\left(i\frac{\pi}{f\lambda}[(x-x_n)^2+(y-y_n)^2]\right)\right|^2 \\ &= A_0^2+2A_0\frac{A_1}{f}\sum_n \cos\left(\frac{\pi}{f\lambda}[(x-x_n)^2+(y-y_n)^2]\right) \\ &\quad +\frac{A_1^2}{f^2}\sum_n \exp\left(i\frac{\pi}{f\lambda}[(x-x_n)^2+(y-y_n)^2]\right)\sum_n \exp\left(-i\frac{\pi}{f\lambda}[(x-x_n)^2+(y-y_n)^2]\right) \\ &\approx A_0^2+2A_0\frac{A_1}{f}\sum_n \cos\left(\frac{\pi}{f\lambda}[(x-x_n)^2+(y-y_n)^2]\right) \end{aligned} \tag{2}$$

where A_0 is reference wave amplitude. Here we use the approximation that $A_1 << A_0$.

After developing and bleaching, we will get a phase hologram [17] and the transmission can be written as

$$\begin{aligned} t(x) &= \exp\left[iK\left(A_0^2+2A_0\frac{A_1}{f}\sum_n \cos(\frac{\pi}{f\lambda}[(x-x_n)^2+(y-y_n)^2])\right)\right] \\ &= \exp(iKA_0^2)\prod_n \exp\left[i\beta\cos(\frac{\pi}{f\lambda}[(x-x_n)^2+(y-y_n)^2])\right] \end{aligned} \tag{3}$$

where K is a constant, and $\beta = 2KA_0A_1/f$ is the modulation amplitude. The modulation term can be further expanded as

$$\exp\left[i\beta\cos(\frac{\pi}{f\lambda}[(x-x_n)^2+(y-y_n)^2])\right] = \sum_{l=-\infty}^{\infty}(i)^l J_l(\beta)\exp[il\frac{\pi}{f\lambda}[(x-x_n)^2+(y-y_n)^2]] \tag{4}$$

where $J_l(\beta)$ is the lth order Bessel function of the first kind. When β is small and $l \geq 0$,

$$J_l(\beta) \approx \frac{1}{\Gamma(l+1)}\left(\frac{\beta}{2}\right)^l \tag{5}$$

Neglecting higher order terms, we have

#128026 - $15.00 USD Received 5 May 2010; revised 27 May 2010; accepted 10 Jun 2010; published 21 Jun 2010

$$\exp\left[i\beta\cos(\frac{\pi}{f\lambda}[(x-x_n)^2+(y-y_n)^2]) \right]$$
$$\approx J_0(\beta)+iJ_1(\beta)\exp[i\frac{\pi}{f\lambda}[(x-x_n)^2+(y-y_n)^2]]+iJ_{-1}(\beta)\exp[-i\frac{\pi}{f\lambda}[(x-x_n)^2+(y-y_n)^2]] \quad (6)$$
$$\approx 1+\frac{i\beta}{2\Gamma(2)}\exp[i\frac{\pi}{f\lambda}[(x-x_n)^2+(y-y_n)^2]]+\frac{i\beta}{2\Gamma(2)}\exp[-i\frac{\pi}{f\lambda}[(x-x_n)^2+(y-y_n)^2]]$$

where we use the relation $J_{-1}(\beta) = J_1(\beta)$. Thus Eq. (3) becomes

$$t(x)\propto\prod_n\left(1+\frac{i\beta}{2\Gamma(2)}\exp[i\frac{\pi}{f\lambda}[(x-x_n)^2+(y-y_n)^2]]+\frac{i\beta}{2\Gamma(2)}\exp[-i\frac{\pi}{f\lambda}[(x-x_n)^2+(y-y_n)^2]]\right) \quad (7)$$
$$\approx 1+\frac{i\beta}{2\Gamma(2)}\sum_n\exp[i\frac{\pi}{f\lambda}[(x-x_n)^2+(y-y_n)^2]]+\frac{i\beta}{2\Gamma(2)}\sum_n\exp[-i\frac{\pi}{f\lambda}[(x-x_n)^2+(y-y_n)^2]]$$

We neglect higher order terms in this analysis. The first term corresponds to the 0 order of the transmitted beam, and the second and third terms correspond to the + 1 and −1 order of the diffraction. Comparing with Eq. (1), we can see that the + 1 and −1 order diffraction will generate the focus grid and its conjugate image. The amplitude of the + 1 order diffraction, which is the diffraction order that we are interested, can be written as

$$\left|\frac{i\beta}{2\Gamma(2)}\right|^2 \propto \beta^2 \propto A_0^2A_1^2/f^2 \quad (8)$$

Thus, the reconstructed focus spot intensity will be proportional to the intensity of reference beam, the intensity of sample beam behind the mask, and inversely proportional to the square of focal length. Note that the above equation is an approximation and is not valid for comparable reference and sample beam intensities.

For the focus spot size, a perfectly reconstructed focus spot will be comparable in size to the original aperture in the mask. However, for small apertures that are comparable to the wavelength, the reconstructed spot size will also depend on other factors, such as the resolution of the holographic material, uniformity of the holographic emulsion, the focal length, and the relative intensity between sample and reference beams.

In the next section, we show the result of a series of experiment, where we fabricated holograms using masks with different ODs, different sizes of the apertures, and different focal lengths. The experimental results agree well with the above theoretical analysis.

3. Experiments and Analysis

In the experiment, we used chrome masks with OD = 2.1, 3.2, 4.2, and 5.3. A line of apertures were punched through the metal film on each mask using focused ion beam, and the sizes of the apertures were 0.2, 0.4, 0.6, 0.8, 1.0, 1.2, 1.4, 1.6, 1.8, and 2.0 μm. The separation between adjacent apertures was 60 μm. For each mask, holograms were recorded at focal lengths of f = 3, 6, 9, 12 mm. We used a green laser with wavelength of 532 nm and power of 200 mW (Excelsior-532-200, Spectra-Physics) for recording the hologram. The holographic material was silver halide (VRP, Integraf). In the reconstruction, we set the intensity of the collimated beam incident on the hologram to be 17 μW/cm^2.

With increasing ODs, the reference beam was attenuated more and the intensity was closer to that of the sample beam. According to the previous discussion, we should expect to see better diffraction and stronger focus spots for larger OD, since the intensities of the sample beam will be more comparable to that of the reference beam. So it is not surprising that for OD 2.1, and 3.2, the reconstructed spots can be observed clearly for all the aperture sizes except 0.2 μm, and for OD 4.2, all the reconstructed spots can be observed. However, for OD 5.3, we can observe multiple diffractions of the hologram, which prevent a clear correspondence between focus spots and the apertures on the mask.

#128026 - $15.00 USD Received 5 May 2010; revised 27 May 2010; accepted 10 Jun 2010; published 21 Jun 2010

Figure 2 shows the microscope image of masks and reconstructed spots of holograms with OD 4.2 and OD 5.3. Figure 2(a), 2(b) show the images for OD-4.2 mask, where the reconstructed spots is an exact replication of the apertures. Figure 2(c), 2(d) show the images for OD-5.3 mask, where we can see that the number of reconstructed spots is more than that of the apertures. This is because for OD 5.3, the interference between the transmissions of different apertures is comparable to the interference between the transmission of apertures and the reference beam. Thus unwanted interference between the aperture transmissions would be patterned onto the hologram and and prevent a clearly reconstruction of the focus spots that correspond to the original apertures. For OD 2.1, 3.2 and 4.2, the intensity of reference beam is much higher than that of the sample beam, and the correspondence of reconstructed focus spots and original apertures can be clearly seen.

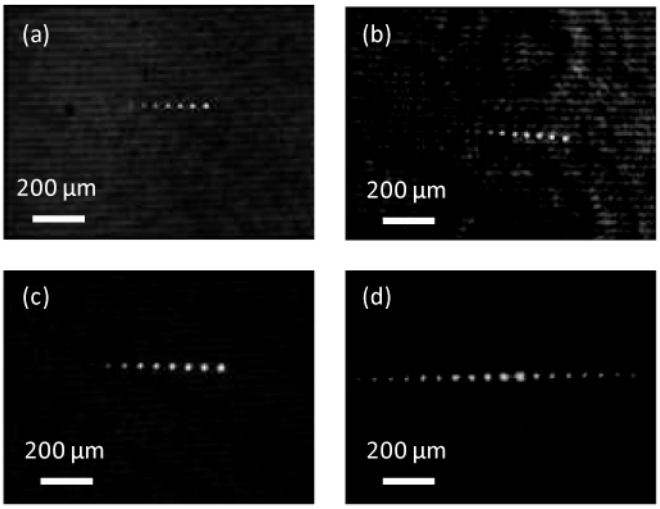

Fig. 2. Microscope image of masks and reconstructed spots of holograms under 4X objective. (a) Mask with OD 4.2; (b) Reconstructed spots of hologram corresponding to OD-4.2 mask; (c) Mask with OD 5.3; (d) Reconstructed spots of hologram corresponding to OD-5.3 mask.

The reconstructed spot intensities and the full-width-half-maximum (FWHM) spot sizes were measured, using a microscope with 60X/NA0.95 objective, for OD 2.1, 3.2, and 4.3 and plotted in Fig. 3, where Fig. 3(a), 3(b) show the plots for OD 2.1, Fig. 3(c), 3(d) show the plots for OD 3.2, and Fig. 3(e), 3(f) show the plots for OD 4.3. From Fig. 3(a), 3(c), and 3(e), we can observe the following important features regarding the reconstructed spot intensity:

(I1) For same OD and same focal length, the reconstructed spot intensity decreases with smaller aperture size. This could be explained by less transmission through smaller apertures and Eq. (8).

(I2) The reconstructed spot intensity is roughly inversely proportional to the attenuation coefficient of reference beam through the mask, and thus stronger for larger OD. This is because in the experiment, the total exposure on the holographic plate is set to be the optimal value of 80 μJ/cm^2 for the holographic material VRP. Assuming that the reference beam intensity is much larger than the sample beam intensity, the increase in OD of the mask will result in increase in sample beam exposure during recording as the exposure time will be longer. Thus according to Eq. (8), the spot intensity will increase to the same amount as OD decreases. The experiment shows that for the same aperture size, the spot intensities of OD-3.2 holograms are roughly 10 times of the spot intensities of OD-2.1 holograms, and the spot intensities of OD-4.2 holograms are roughly 5-8 times of the spot intensities of OD-3.2 holograms. This agrees well with the theory

#128026 - $15.00 USD Received 5 May 2010; revised 27 May 2010; accepted 10 Jun 2010; published 21 Jun 2010

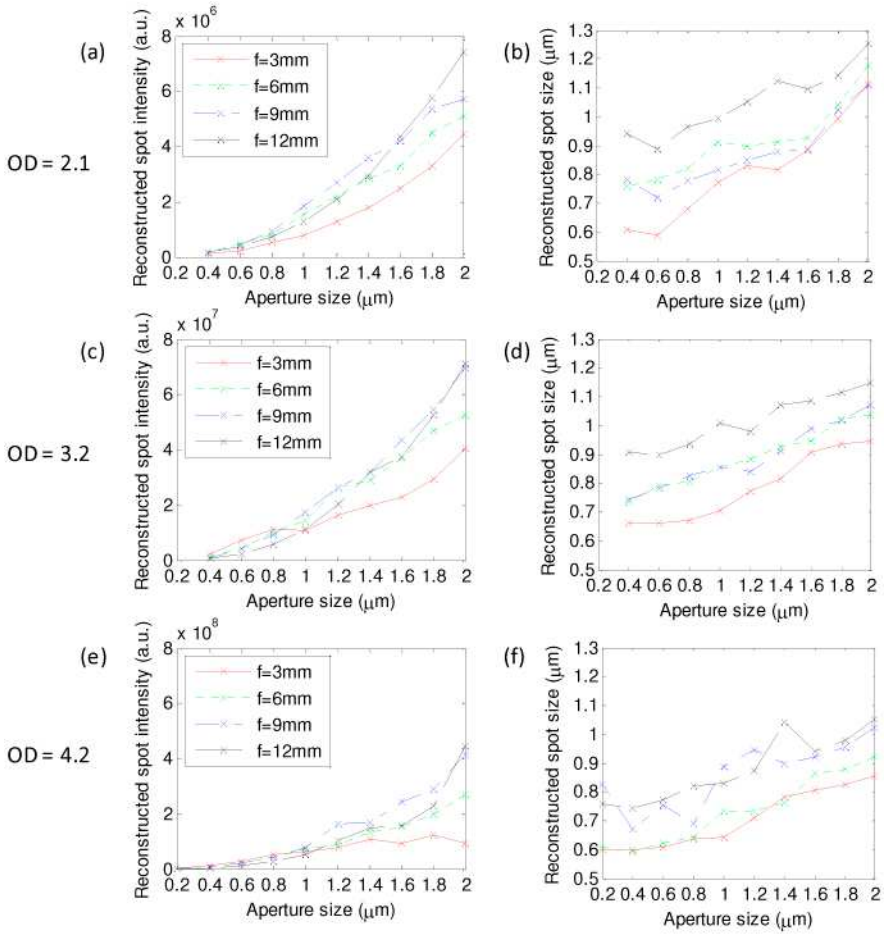

Fig. 3. Reconstructed spot intensity and FWHM spot size versus aperture size at different ODs and different focal lengths. (a)(b) OD = 2.1; (c)(d) OD = 3.2; (e)(f) OD = 4.2.

From Fig. 3(b), 3(d), and 3(f), we can observe the following important features regarding reconstructed spot size:

(S1) For same OD and same aperture, the spot size decreases with smaller focal length. This could be explained by the effective holographic lens area on the hologram. As the focal length decreases, the effective holographic lens area also decreases, thus the impact of possible non-uniformity of the holographic recording material on the lens quality would be less, and the reconstructed spot size can be closer to the original aperture size.

(S2) For same OD and same focal length, the spot size decreases with smaller aperture size and finally reaches an asymptotic value. The decrease in spot size is consistent with our logical expectation. The existence of an asymptotic value is unsurprising as well – the holographic material can only record feature size down to a certain limit. Reconstruction of a small spot requires the patterning of finer diffraction features. Once we have reached that limit, we cannot expect the reconstruction spot size to taper to an asymptotic value and any further decrease in the mask's aperture size would have no impact.

#128026 - $15.00 USD Received 5 May 2010; revised 27 May 2010; accepted 10 Jun 2010; published 21 Jun 2010

We can see that the reconstruction spot can have an FWHM spot size as small as 0.6 μm. Note that this can be smaller than the aperture diameter since we measured the FWHM spot size, which was related to the diffraction of the aperture.

(S3) For different OD and same aperture size, we can obtain similar reconstructed spot size, especially for small apertures and small focal lengths. This indicates that the spot size is less sensitive to the relative intensity between reference and sample beam, and more depending on the effective holographic lens area. This implies that the uniformity of the holographic material is an important quality-determining factor.

According to these experimental observations, we can see that to get an optimal hologram quality, we would first need to choose an optimal OD for the mask. An OD of 4 works well for holographic grid designs that are similar to the one we have here. We note that choosing an OD beyond 4 can potentially provide even better efficiency. However, an excessively high OD would significantly attenuate the reference intensity. In our experiments, the direct transmission through the mask becomes exceedingly weak for an OD beyond 5. In this situation, the diffraction transmissions through adjacent apertures would interfere significantly and lead to significant cross-talks.

Next an appropriate aperture size should be chosen according to (I1) and (S2), which show that there is a trade-off between spot intensity and spot size. Finally we can see that for small apertures, the spot intensity and spot size will generally get better as focal length decreases, thus we would want to choose the smallest possible focal length as long as it is compatible with the system design.

In the fabrication of our demonstration focus grid, we chose to use an aperture size of 0.8 μm for small enough reconstructed spot size based on the reasons listed above. Figure 4 shows the reconstructed spot intensity vs. focal length and OD for the 0.8-μm aperture size. We can see that there is an optimal parameter set for getting the best spot intensity.

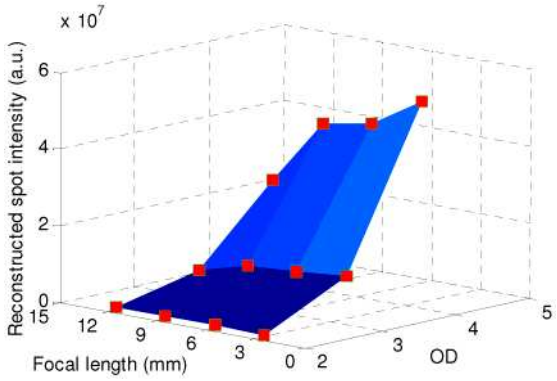

Fig. 4. Reconstructed spot intensity vs. focal length and OD for 0.8-μm aperture size. The squares indicate the experiment data points.

Using the in-line holography method, we fabricated a hologram that can generate a focus grid of 170 x 138, with 30-μm separation between the focus spots. The hologram was recorded with an OD 4 mask with apertures of 0.8-μm diameter, and at a focal length of 5 mm. Figure 5 shows a small part of the reconstructed spots observed under microscope with a 20X objective. The FWHM spot size was measured to be around 0.7 μm. The focus grid can be readily used in a wide-field microscope system.

#128026 - $15.00 USD Received 5 May 2010; revised 27 May 2010; accepted 10 Jun 2010; published 21 Jun 2010

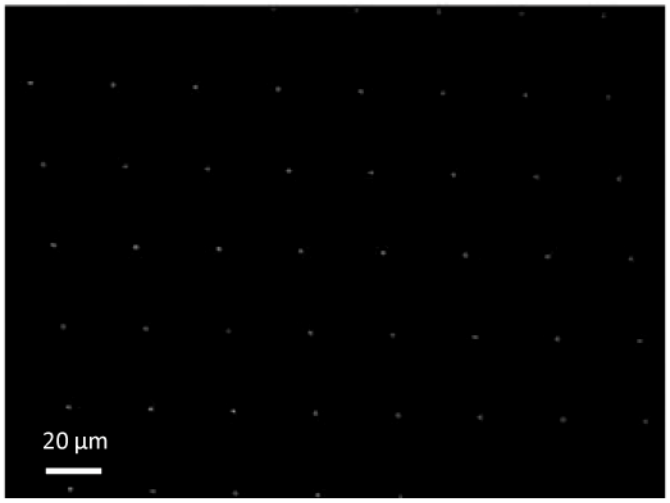

Fig. 5. Microscope image of a small part of the reconstructed focus grid under a 20X objective.

While this set of experiments did not study the impact of aperture separation on the focus grid quality, the observed dependency trends of the other design parameters can help inform us on this relationship. Specifically, an increase in grid density would lead to higher total transmissions through the apertures. This in turn would lead to more interference between the transmissions through different apertures. In this case, we expect a lower OD mask would be required so that the in-line holography interference is stronger than the cross-talk terms. The exact impact of aperture separation is well worth a future detailed experimental study.

4. Summary

In conclusion, we have shown an in-line holography scheme for recording a hologram to generate a wide-area focus grid. Compare with other methods for generating focus grid, our scheme is relatively simple, robust, and have many other advantages. We have studied the effect of mask OD, aperture size, and focal length on recording process and showed that a set of appropriate parameters is important for fabricating the hologram. A hologram was fabricated to generate a wide-area focus grid for demonstration of principle. The hologram can be potentially used for wide field-of-view imaging or parallel detecting and sensing applications.

Acknowledgement

The authors acknowledge Ying Min Wang, Guoan Zheng, and Dr. Xiquan Cui for helpful discussions. This work is supported by Department of Defense grant #W81XWH-09-1-0051.

#128026 - $15.00 USD Received 5 May 2010; revised 27 May 2010; accepted 10 Jun 2010; published 21 Jun 2010